ISSN: 0067-2904
GIF: 0.851

Basin or Intrusion, a New Method to Resolve Non-Uniqueness in Gravity Interpretation

Ali M. AL-Rahim[1*], Williams A. Lima[2]
[1]Department of Geology, College of Science, University of Baghdad, Baghdad, Iraq
[2]Universidade Federal do Pará, Programa de Pós-graduação em Geofísica CG, Belém, Brazil

Abstract

The aim of the current paper is to resolve the non-uniqueness in gravity interpretation through searching for singular points in the gravity field that are coincide with causative body vertices. The Absolute Second Horizontal Gradient (ASHG) method is used to locate the horizontal reference location of the body, while its amplitude could be used to define body corner depth. Intelligent use of the ASHG method could help in differentiating between basin and intrusion structures from their gravity effect and could facilitate the interpretation in forward modeling and constrain inversion modeling to maximum limit. The method is tested by using many synthetic examples with different types of shapes. A real data is used to examine the method and give a decisive result about the type and shape of the causative body.

Keywords: Absolute Second Horizontal Gradient (ASHG), Singularity, Restricted Inversion, Gravity Interpretation.

حوض ام اقحام ، طريقة جديدة لحل عدم – التفرد في تفسير الجاذبية

علي مكي حسين الرحيم[1]*، وليام أي ليما[2]
[1]قسم علم الارض، كلية العلوم، جامعة بغداد، بغداد، العراق
[2]الجامعة الاتحادية، البرازيل

الخلاصة:

هدف الدراسة الحالية هو لحل عدم التفرد في التفسير الجذبي من خلال البحث عن نقاط وحيدة في المجال الجذبي والتي تتطابق مع حواف الاجسام المسببة للمجال. طريقة المشتقة الافقية المطلقة الثانية استخدمت لايجاد المواقع المرجعية للجسم في حين يمكن استخدام سعاتها لتحديد اعماق اركان الجسم. الاستخدام الماهر للمشتقة الافقية المطلقة الثانية يمكن ان يساعد في المقارنة بين التراكيب الحوضية والاقحامية من مجالها الجذبي وهذا يمكن ان يسهل من عمل النمذجة المباشرة ويقيد النمذجة المعكوسة الى اقصى حدودها. الطريقة اختبرت على نماذج ممثلة بعدة انواع واشكال لمصادر جذبية وكذلك تم اختبار الطريقة على بيانات حقيقية واعطت نتائج حاسمة حول نوع وشكل الجسم المسبب للمجال.

Introduction:

The interpretations of gravity data suffer from non-uniqueness in solution where bodies with different shapes can produce exactly the same anomalies. In such a case, it is not possible to deduce a unique body from an anomaly in spite of the possibility to calculate unique anomaly due to any specified body. This problem (in addition to uncertainties arising from poor or sparse data, or interference from other anomalies) makes modeling even more difficult. Mussett and Khan [1, page 120, Figure 8.17b] give an example for non-uniqueness solution for gravity modeling where basin and intrusion models both have the same gravity anomaly. Another example is given by [2] for interpret a minimum Bouguer gravity survey in the Moray Firth (north-east Scotland) as being due to a granite

*Email: alial_rahim@yahoo.com

pluton. After further geological and gravity works, it was realized that this minimum was due to a sedimentary basin.

Negative gravity anomalies are associated with granite plutons and with sedimentary basins with comparable gravity magnitude and both of them have wide long wavelength anomalies. So, the application of power spectrum depth estimation for both cases will give the same results. Even inversion methods for depth estimation will face the same problem. But the potential gravity field hides some criteria; if used wisely could solve and answers many question regarding the type and shape of the causative body. This criterion is the gradient of the field. Finding the location of steep gradient could help the interpreter to decide the type and shape of the causative body.

This problem was known in geophysical aspect. Bott [3] proposed a set of criteria to distinguish between a sedimentary basin and a granite boss as interpretation of gravity minima. His solution was based on the second vertical derivative of gravity anomaly due to a semi-infinite two-dimensional horizontal slab with a sloping edge. Some authors [4 and 5] search for the location of inflection points on gravity profile (positions where the horizontal gravity gradient change most rapidly). This location can provide useful information on the nature of the edge of an anomalous body. Over structures with outward dipping contacts such as granite bodies, the inflection points lie near the base of the anomaly. Over structures with inward dipping contacts such as sedimentary basins, the inflection points lie near the uppermost edge of the anomaly.

In forward modeling, the gravity field for a created causative body is calculated. The reference locations values of a causative source body vertices or corners are defined in (x,y) coordinate, where (x) define the horizontal reference location while (y) represent its depth. The question now, is it possible to determine the reference location of the causative body corners from its gravity filed. What and where are the singular points in this gravity filed that’s have the ability to located the body corners.

The objective of the current study is to use the concept of Absolute Second Horizontal Gradient (ASHG) for the gravity field in 1D and 2D as a new diagnostic purpose tool to determine the exact horizontal reference location (x) for body vertices that produces the gravity field. The presented solution is based on the use of ASHG for a gravity field produced from line source with a sloping edge. The tool will be used latter to distinguish between sedimentary basin and granitic pluton or intrusion structure. Then the maximum magnitude values of ASHG will be used to define depth of body vertices beside other tools used for the same purpose. The method is tested on synthetic gravity anomalies due to different source bodies. Constrain inversion method is applied for a synthetic basin model data to insure the fidelity of the tool. Later on, the method is examined real gravity data to distinguish whether these anomalies are related to basin or intrusion structure.

Theoretical background:

Singularities of potential field:

Every potential field must possess singularities somewhere in the entire space; otherwise, the potential field will be zero everywhere. The singularities are the only points where the potential is maximum (or minimum). Since the potential field cannot possess a singularity in the free space, all singularities must be confined to the interior or at the most on the surface of the source. It must be pointed out that the singularities are encountered only when the external potential field is analytically continued into the region occupied by the source. The importance of the singularities lies in the fact that these can be uniquely determined from the observed field. They are often closely related to the shape parameters of the source [6].

By definition, the singularities are points where a function ceases to be analytic. Such points are precisely the points where physical sources which give rise to potentials are located [7]. Singular points in a complex plane may be poles, zeros, essential singularities or branch points [8].

Each singular point of the gravity field for a body source is described by three sets of parameters namely: location, amplitude and order of singularity. A group of singularities associated with a source may be enclosed by a convex surface. Often, it is the top most singular point on the convex surface which is of great interest, and it is also the one which can be determined relatively easily. The exact location of maximum value (singular point) of the field could be determined using derivative (Gradient) method [6].

Mathematical concepts:
Absolute Horizontal Gradient (AHG):
For a profile (1D):
If g(x) is the gravity field in x direction then its absolute horizontal gradient is:

$$(AHG_{1D}) = \left|\left(\partial g / \partial x\right)\right|$$

The Absolute Second Horizontal Gradient ($ASHG_{1D}$) to (AHG_{1D}) is:

$$ASHG_{1D} = \left|\left(\partial AHG_{1D} / \partial x\right)\right|$$

The latter ($ASHG_{1D}$) is equal to the value of Absolute Second Derivative (ASD_{1D}) for the gravity field:

$$ASD_{1D} = \left|\partial^2 g / \partial x^2\right| = ASHG_{1D}$$

For a map (2D): If g(x,y) is the gravity field in two dimension and the horizontal derivatives of the field are $\left(\partial g / \partial x\right)$ in x direction and $\left(\partial g / \partial y\right)$ in y direction, then the horizontal gradient (HG_{2D}) in (x,y) direction is given by:

$$HG_{2D}(x,y) = \left(\left(\partial g / \partial x\right) + \left(\partial g / \partial y\right)\right).$$

The Gradient Operator with the following formula is used to eliminate the sign effects of the $HG_{2D}(x,y)$ values due to the direction of calculating the horizontal gradient in two direction:

$$\left|HG_{2D}(x,y)\right| = \sqrt{\left(\frac{\partial g}{\partial x}\right)^2 + \left(\frac{\partial g}{\partial y}\right)^2} = AHG_{2D}$$

The Gradient Operator generates a grid of steepest slopes (i.e. the magnitude of the gradient) at any point on the surface. The Gradient Operator is zero for a horizontal surface, and approaches infinity as the slope approaches vertical.

Applying horizontal gradient again to the last data $|HG_{2D}(x,y)|$ and take its absolute values will produce the Absolute Second Horizontal Gradient ($ASHG_{2D}$) which is given by:

$$ASHG_{2D} = \left|\left(\partial\left|HG_{2D}(x,y)\right| / \partial x\right) + \left(\partial\left|HG_{2D}(x,y)\right| / \partial y\right)\right|$$

Again, using the absolute is to eliminate the sign effects of the values due to the direction of calculating the horizontal gradient.

The $ASHG_{2D}$ is equal to the absolute second derivative (ASD_{2D}) of the original data and the absolute Laplacian operator $\left|\nabla^2 g\right|$ with the following formula can apply and explain this concept:

$$\left|\nabla^2 g\right| = \left|\frac{\partial^2 g}{\partial x^2} + \frac{\partial^2 g}{\partial y^2}\right| = ASHG_{2D} = ASD_{2D}$$

The Gradient and Laplacian operators are easy to be determined in SURFER POGRAM, V.12 [9]. The user needs only to convert the Laplacian output to its absolute value using Math order and (fabs) function which is built-in function in Surfer program.

As state earlier, the Gradient and Laplacian operators requires computation of absolute horizontal derivatives of the first and second orders. It is a well-known fact that the filter characteristics of these derivatives are essentially high-frequency enhancement filters. Due to this characteristic, any high frequency noise presents in the data and any white noise in the map due to digitization error get substantially enhanced, masking the response from the target. For that, smoothing the gravity map before processing the Gradient and Laplacian operators is mandatory to remove the effect of high frequencies present in the observed data and to enhance the signal to noise ratio.

The smoothing approach utilized in this study is done by using the concept of linear convolution filter in image processing as a low-pass moving average filter with kernel dimension 5x5 with the following parameters [10, 11]:

1	1	1	1	1
1	1	1	1	1
1	1	1	1	1
1	1	1	1	1
1	1	1	1	1

Constrain modeling and inversion by using line integral $\int$ concept:

Actually, each vertex reference location derived from the ASHG profile could be used to constrain the modeling and inversion procedure to follow the source body geometry. That is related to the mathematical formula used in 3D modeling programs which includes conversion of the volume integral $\iiint$ of the causative body to a summation of lines integral $\int$ for the lines that bound the boundary of the body to make the numerical computation procedure easier and simplified. The same is for 2D modeling, where the conversion includes converting surface integral $\iint$ to a lines integral $\int$ that's make the boundary of the causative bodies [12-15]. This concept is a part of Green theorem to facilitate the computation of the gravity effect of the causative bodies [16].

Blakely [17] and Roy [7] expressed the formula used in forward modeling the gravity anomaly for a body has any number of sides with assumed homogeneous physical properties. Their expression for gravity field is derived from the fields of 2D N-side polygon. When N=3 (Figure-1) the gravity anomaly of triangular ΔABC at observation point O is expressed as:

$$\Delta g_j = \sum_{i=1}^{3} \delta g_i = 2G\Delta\rho \sum_{i=1}^{3} \frac{\xi_i \zeta_{i+1} - \xi_{i+1}\zeta_i}{(\zeta_{i+1} - \zeta_i)^2 + (\xi_{i+1} - \xi_i)^2}$$

$$\left[(\xi_{i+1} - \xi_i)\left(\tan^{-1}\frac{\zeta_i}{\xi_i} - \tan^{-1}\frac{\zeta_{i+1}}{\xi_{i+1}} \right) + \frac{1}{2}(\zeta_{i+1} - \zeta_i)\ln\frac{\xi_{i+1}^2 + \zeta_{i+1}^2}{\xi_i^2 + \zeta_i^2} \right]$$

Where: Δg_j is the gravity anomaly of the jth triangle cell, δg_i is the gravity anomaly caused by the ith edge of the triangle, G is the gravity constant, $\Delta\rho$ is the density contrast, (ξ_i, ζ_i) is the coordinate of the ith triangle corner.

Adding the gravity anomalies caused by all triangle cells, the gravity anomalies (i.e., Δg) of the 2D arbitrary shape model are written as:

$$\Delta g = \sum_{j=1}^{N_T} \Delta g_j$$

Where: N_T is the number of the triangular cells.

The reference cells location in x direction for the triangle body could be determined by applying the ASHG method to its gravity field as will be proven in the synthetic examples later on. These reference locations can be uniquely determined from the observed field due to singularities properties of their fields. They are related to the shape parameters of the source.

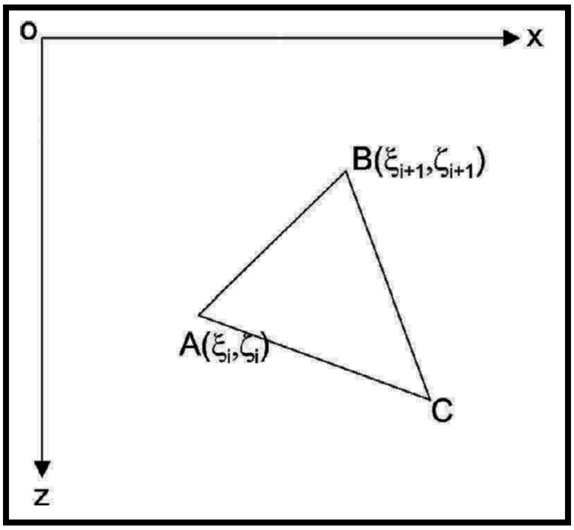

Figure 1- Diagram of triangle cell

Applied the AHG and ASHG:

The Absolute Horizontal Gradient (AHG) and the Second Absolute Horizontal Gradient (ASHG) are calculated for gravity anomalies due to different source bodies and can be seen in Figure-2 (Black colour for gravity, Blue for AHG and Red for ASHG).

The gravity field for vertical contact line source has single point of maxima in AHG profile with symmetrical bell shape. The ASHG profile shows zero value directly over the contact (coincided with the maximum value of AHG profile) with symmetrical maximum amplitude values on both side of the zero point Figure-2a.

The square root of the AHG plus the absolute vertical gradient makes what is called Analytical Signal [18-20]. Nearly all automatic basement depth estimation methods assume that the basement block has vertical contact and the maximum values of AHG and/or Analytical Signal can be used as a tool for depth estimation [21-29]. But, this is not valid in many cases of basement that has listric or dipping faults. The line that resemble the dipping fault has two vertices, and these vertices sign their signature on the AHG as a steep slope with asymmetrical bell shape, while the ASHG profile gives maximum values which have two relative different amplitudes over these vertices with asymmetrical amplitude maximum values on both side of the zero point Figure-2b. Thus, the ASHG is a diagnostic method to find the horizontal reference location of body vertices.

Actually and for historical documentation, the gradient steep slope across the edge of dipping layer is known since 1927, where Heiland [30] exhibited Figure-3 related to (Jung, Zeit. *Geophys.*, 3(6), 267-280 (1927)). The G and K in Figure-3 were representing the Gradient and Curvature values respectively.

Now, if the second vertex of the body is deeper (Down dip) then the maximum amplitude of their ASHG is lower. If the second vertex of the boy is shallower (Up dip) then the maximum amplitude of their ASHG is relatively higher. Many types of structures are modeled and their AHG and ASHG are calculated (Figure-2c, d, e, f, g, h). The (x) locations of maximum values of ASHG in the figures of these models are coinciding directly over the vertices of the causative bodies. Special attention should be considered to the models of the basin and intrusion (Figure-2i and j). The ASHG for the basin has very high amplitude on both sides of the basin and low values in its mid part. While, for intrusion body; the ASHG has low amplitude on both sides and high values in its mid part. Therefore, it is possible to conclude whether the negative anomaly is produced from basin or intrusion. Also, it can make a comparison between the vertical contact and dipping one (Figures-2e and h). These criteria could help the interpreter to know exactly the geological case dealing with and determine the exact horizontal reference location of the faults. This will increase dramatically the facility of modeling and constrain inversion process for these structures and give the inversion more reality besides, it reduces the non-uniqueness in the interpretation of gravity data.

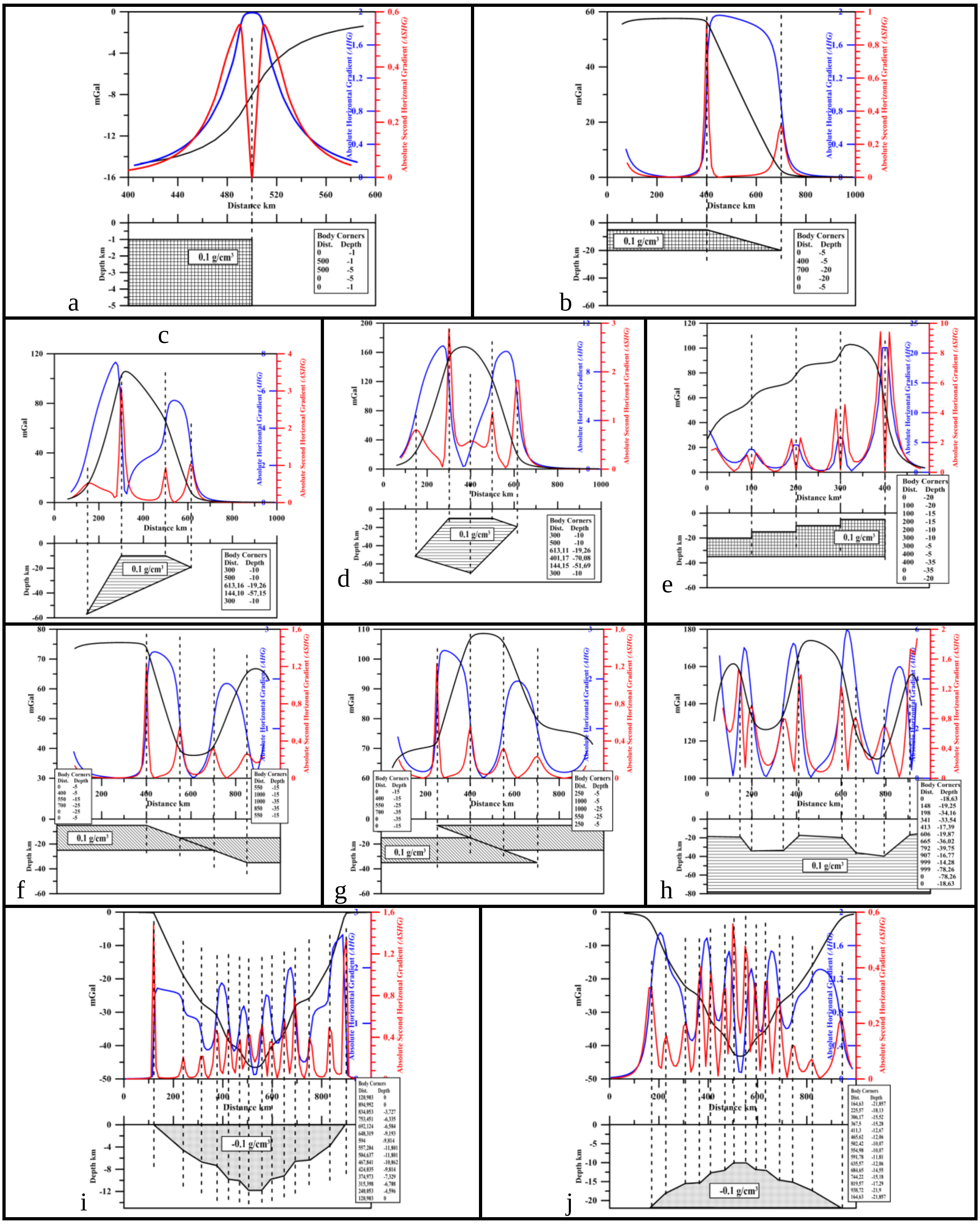

Figure 2-Application of AHG and ASHG to the gravity field for different types of bodies. (Black colour = gravity, Blue colour= AHG and Red colour = ASHG).

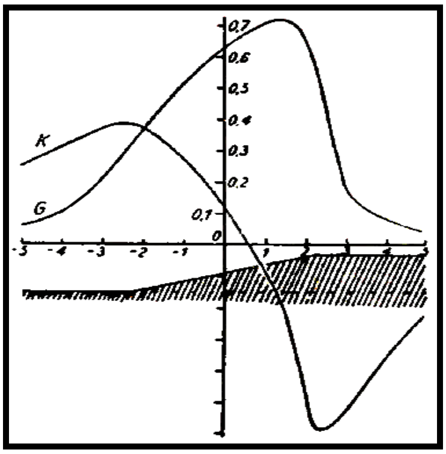

Figure 3- The G and K curves are represents the Gradient and curvature values respectively. (After [30])

Now, what about flatten sedimentary beds cases. Actually, their gravity field will be constant (their gravity are from slab formula = 2πΔρGh, depend on their parameter values of the depth (h) to the middle part of the thickness of bed, the density contrast Δρ and G the gravitational constants) and does not analytic with respect to x direction. Therefore; the flatten beds have no singular point in any locations across the surface of the beds.

Depth Estimation and gravity inversion:

Locating the horizontal locations of the vertices will greatly help in calculating depth of the source body at this location form their gravity filed. Different methods for estimating depth could be dependent on:

1) Simple method to estimate the depth (h) to the center of the slab thickness from their gravity value is by using slab formula: g = 2πΔρGh

Where: g is the gravity value, G is the Gravitational constants and Δρ is the density contrast.

2) Bott [31] was presented the following very fast, iterative method to estimate the depth to the basement relief $p(x_i)$ of a sedimentary basin, where $x_i, i = 1,....., N$ is the set of horizontal coordinates of the N gravity observations $g^o(x_i), i = 1,......, N$. At the kth iteration (k≥1), the approximation $p^k(x_i)$ is given by:

$$p^k(x_i) = p^{k-1}(x_i) + \frac{g^o(x_i) - g(x_i, \Delta\rho, p^{k-1})}{2\pi\gamma\Delta\rho}, i = 1,...., N$$

Where: γ is the gravitational constant, Δρ is the density contrast (presumed constant and known) between the sediments and the basement, and $g(x_i, \Delta\rho, p^{k-1})$ is the computed gravity anomaly at x_i produced by an interpretation model. Careful inspection for Bott [31] formula shows that this formula is like the slab formula put presented in different manner.

3) Dobrin and Savit [16] estimate the depth *z* to the center *t* of fault slab from the gradient of the gravity anomaly at the point where it is steepest. When all distances are in thousands of feet, the gradient of g_z with respect to *x* is:

$$\frac{dg_z}{dx} = 12.77\rho \frac{t}{\pi} \frac{1}{z} \frac{1}{1 + (x/z)^2}$$

The required slope can be obtained from the graph of AHG where the gradient has maximum value. This maximum slope coincides with a maximum peak on the ASHG graph. Determining this location will prevent the error and human bias in calculating the required slope.

4) So that, the proposed method in the current paper by using ASHG, the depth can be calculated at the point of maximum value of the ASHG using the second derivative of the above formula with respect to *x* that is:

$$\frac{d^2 g_z}{dx^2} = 12.77\rho \frac{t}{\pi} \frac{1}{z^3} \frac{-2x}{\left(1 + (x/z)^2\right)^2}$$

Figure-4 shows the result of a modified constrain GUI-MATLAB code [32] prepared for inversion basin structure that had been used by Bott [31] method for a synthetic model. The prepared basin model is similar to a basin model presented by [33]. The horizontal locations of maximum values in ASHG greatly guide the inversion process (Green colour in the figure). The result of the inversion is congruent completely with the model shape, depth and dimension. Thus, determining the horizontal reference locations of the body vertices could reduce the number of iterations, reduce the time for inversion, restrict the morphological shape of the source body and finally gives primer agile assumption for the shape of the body.

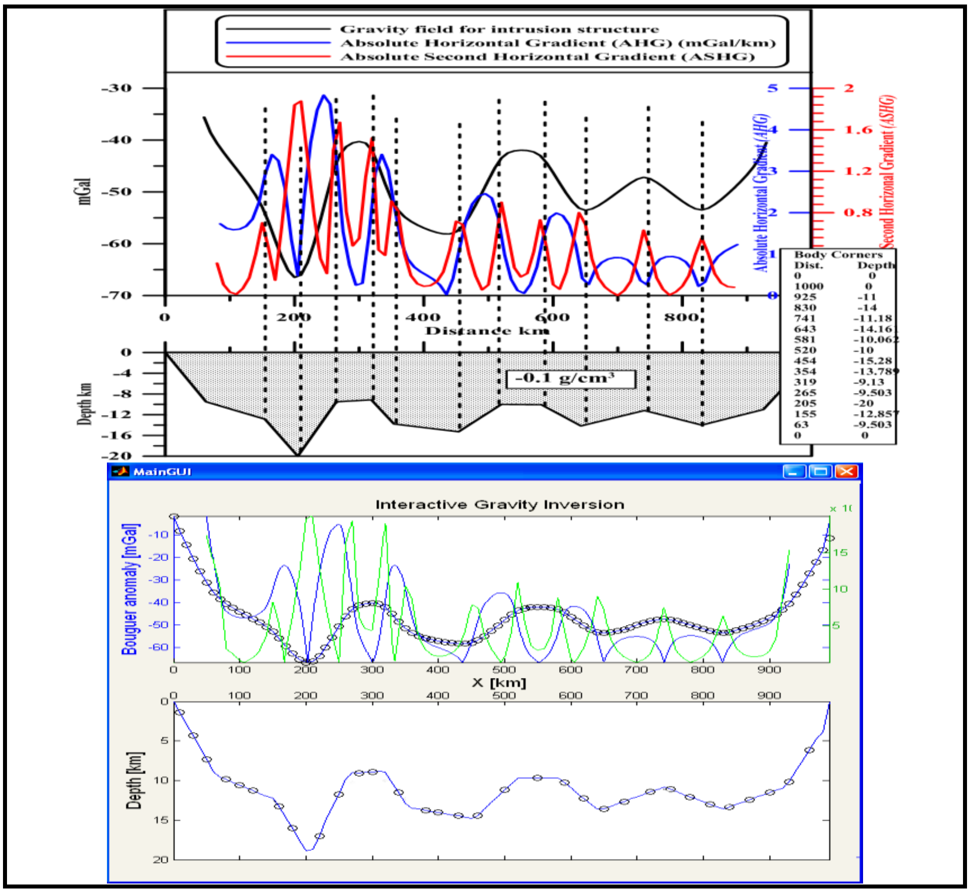

Figure 4-A modified constrain of the GUI-MATLAB code given by [32] that had been prepared for inversion basin structure used by Bott [31] method for a synthetic model. The prepared basin model (above) is similar to a basin model presented by [33].

Examine the method of ASHG for (Basin or Intrusion) real data to decide the type of the source:

The Bouguer gravity field of Iraq [after 34] has been digitized with gird interval 2.5 km Figure-5a. The gravity map shows two major gravity lows separated by a major central gravity high. Tectonically, this area is dividing the territories of Iraq into stable (in the west) and unstable (in the east) shelves. Our test will be concentrate on the stable shelf part area where a wide circular shape anomaly located in the middle part of the stable shelf. Two profiles are selected across this anomaly namely N-S and W-E profiles Figure-5b. Another remarkable enclosed positive gravity anomaly is located at the north of the stable shelf and a profile named A-A' is selected across this anomaly Figure-5b. The third profile named B-B' is selected across a depression area (Maa'niyah depression) that is located at the border with Saudi Arabia Figure-5b. Figures-5c and d show maps represent the process of 2D AHG and ASHG Data.

Figures-6a, b, and c show a zoom maps for the wide circular shape anomaly extracted from Figure-5 with their 2D AHG and ASHG maps. The extractd profiles (N-S, W-E, A-A' and B-B') from these maps Figure-5 and 6 is shown in Figure-7.

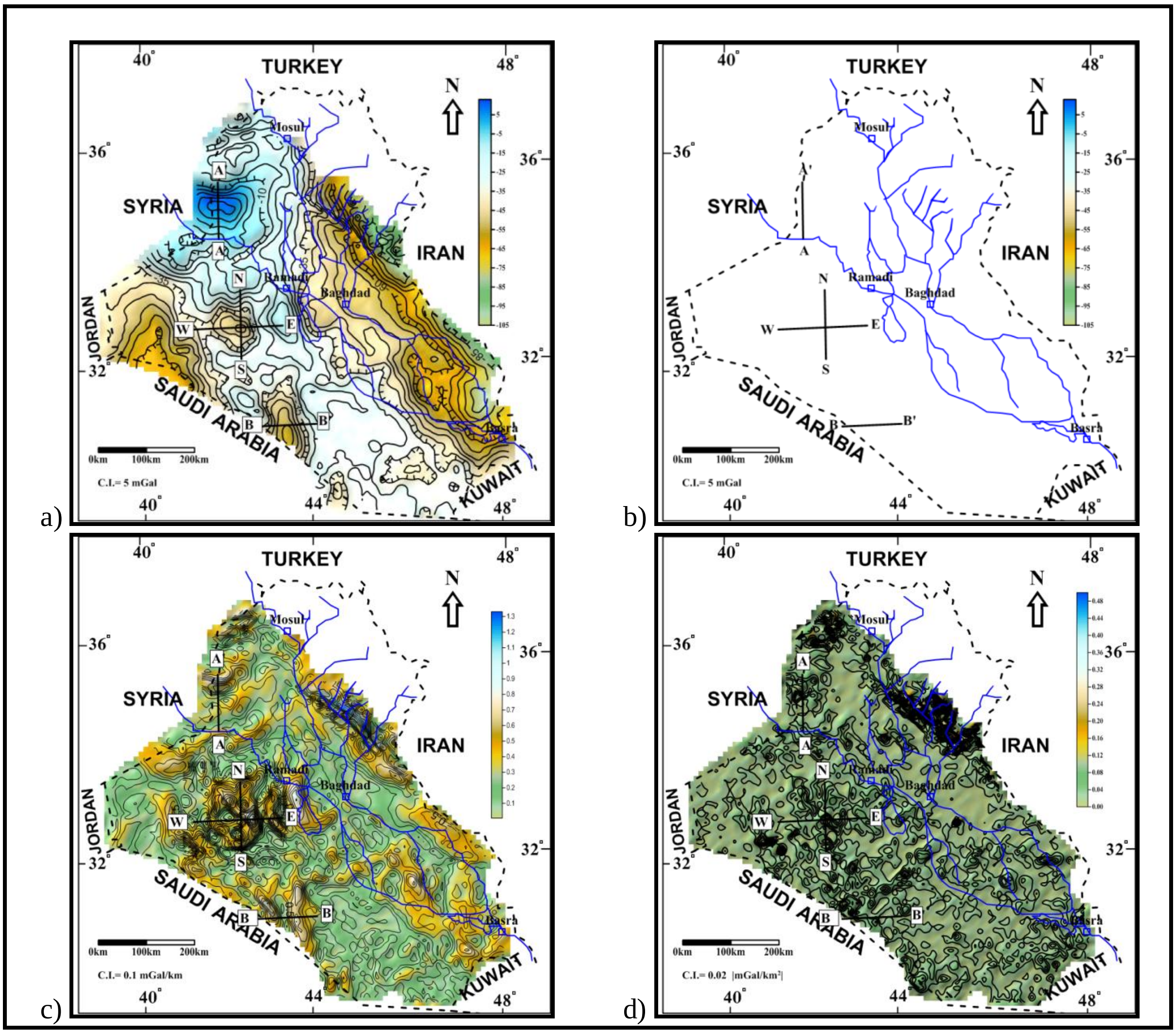

Figure 5-Maps of a) Gravity data of Iraq [34]. b) Profiles of study area. c) Absolute Horizontal Gradient Data. d) Absolute Second Horizontal Gradient Data (Laplacian data).

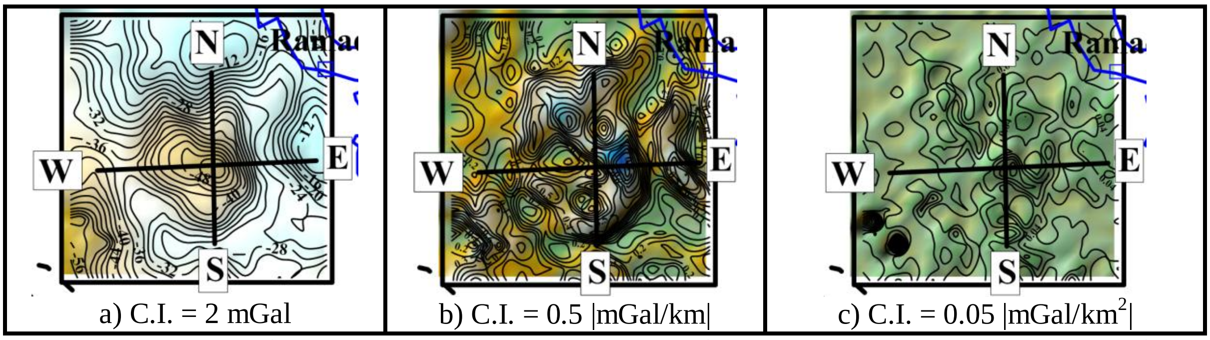

Figure 6- Zoom maps for the circular shape anomaly extracted from Figure-5. a) Gravity map extracted from Figure-5a. b) AHG map extracted from Figure-5c. c) ASHG map extracted from Figure-5d.

Examining the results for the profiles N-S and W-E of the circular shape anomaly Figure-7 showed that the figure is akin to or having similar character of Figure-2j. The source has an intrusion character where the ASHG shows high amplitude in the middle part and low in the side. Some authors interpret this circular anomaly as a basin with salt body of Infracambrian age [35, 36]. Al-Yasi [37] interprets this anomaly as a granitic intrusion. Actually, no well is drilled in this area and no deep seismic exploration is also done, but the result here supports the interpretation of Al-Yasi [37] as the magnetic data has high amplitude values in the same area. Baban [38] presents a figure for regional seismic line cross the same area in W-E direction. The shallow to intermediate reflectors on the presented figure show some antiform shape and may reflect a drape fold.

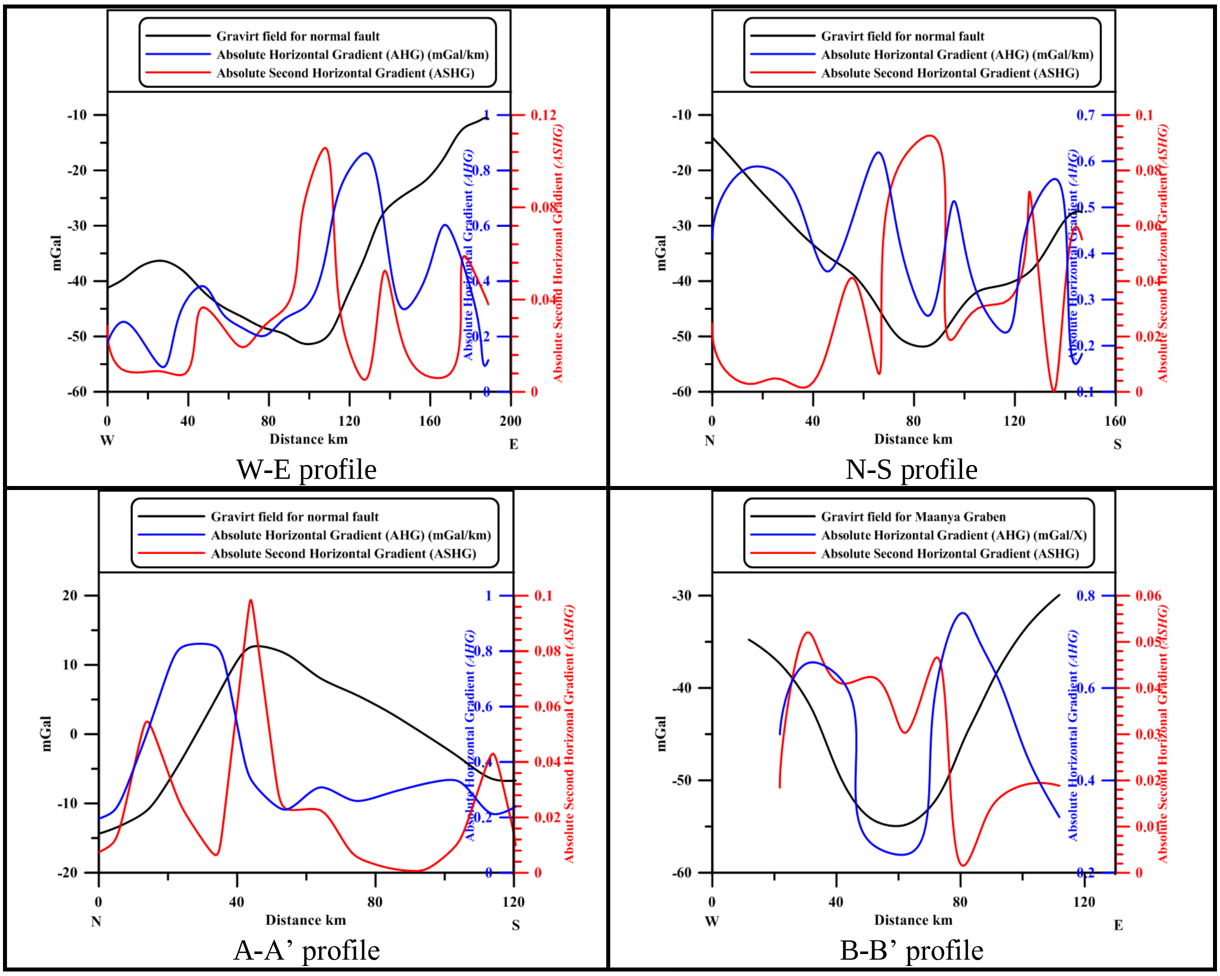

Figure 7- The extracted profiles (N-S, W-E, A-A' and B-B') from maps shown in Figure-5.

The A-A' profile for positive gravity value anomaly Figure-7 shows very sharp and high amplitude in the middle part of the anomaly and low outside with relative different amplitude. The high positive gravity anomaly suggests deep crust-mantle Moho uplift. A forward modeling with ASHG constrain could explain the result.

The profile B-B' Figure-7 support the basin source of Ma'aniyah depression, where the middle part of the anomaly has less amplitude relative to side parts of the anomaly and having similar character of Figure-2i.

Conclusion and discussion:

The current study is a step forward to reduce the non-uniqueness in the interpretation of gravity data and to reduce the illness of gravity inversion. The developed method here is accurate, decisive and practical to estimate the reference of source body vertices. The ASHG method is greatly help the interpreter to use the shape of the anomaly in deciding whether the long wavelength negative anomaly is related to sedimentary basin or granitic intrusion. The validity of the method is proven from the result of using many synthetic data due to various sources of gravity anomalies. The method could be used in gravity inversion to constrain the morphological shape of the basin, reduces the inversion time and the number of iterations. Thus that, the method of ASHG could be used to reduce the non-uniqueness in the interpretation of gravity data.

Reference:

1. Mussett, A. E., and Khan, M. A. **2009**. *Looking into the Earth an introduction to geological* geophysics. Cambridge University press. p:494.
2. Reynolds, J. M. **1997**. *An introduction to applied and environmental geophysics*. Wiley, New York. p: 720.
3. Bott, M. P. H. **1962**. A simple criterion for interpreting negative gravity anomalies, *Geophysics*, 27(3), pp:376-381.

4. Kearey, P., and Brooks, M. **1991**. *An introduction to geophysical exploration*, Second Edition. Blackwell Scientific, Oxford, UK. p:281.

5. Butler, G.K. **1984**. Microgravity and gravity gradient techniques for detection of sub-surface cavities. *Geophysics*, 49(7), pp:1084-1096.

6. Naidu, P.S. and Mathew, M. P. **1998**. *Analysis of Geophysical Potential Fields a Digital Signal Processing Approach*. Elsevier. The Netherlands. p:311.

7. Roy, K.K. **2007**. *Potential Theory in Applied Geophysics*. Springer-Verlag, Berlin Heidelberg, New York. p :660.

8. Spiegel, M.R. **1964**. *Complex Variables, Theory and Problems*, Schaum Publication Co. (Schaum’s Outline Series), New York. p:313.

9. Surfer Program Version 12. **2014**. Surface Mapping System: Golden Software, Inc.

10. Pitas, I. **2000**. *Digital Image Processing Algorithms and Applications*, John Wiley and Sons, New York, p:419.

11. Wiggin, Ender. **2001**. Elementary Digital Filtering: http://www.gamedev.net/ reference/articles/article1068.asp, (09/20/2001).

12. Talwani, M. and Ewing, M.**1960**. Rapid computation of gravitational attraction of 3D bodies of arbitrary shape: *Geophysics*, 30(1), pp:203-225.

13. Götze, H. and Lahmeyer, B. **1988**. Application of three-dimensional interactive modeling in gravity and magnetic: *Geophysics*, 53(8), pp:1069-1108.

14. Bijendra, S. and Guptasarma, D. **2001**. New method for fast computation of gravity and magnetic anomalies due to arbitrary polyhedral: *Geophysics*, 66(2), pp:521-526.

15. Pignatellia, A., Nicolosia, I., Carluccioa, R., Chiappinia, M. and Von Freseb, R.**2011**. Graphical interactive generation of gravity and magnetic fields: *C&G*, 37(4), pp:567-572.

16. Dobrin, M. B. and Savit, C. H.**1988**. *Introduction to geophysical prospecting*: McGRAW-HILL book company, Fourth Edition. p:883.

17. Blakely, R.J. **1996**. *Potential Theory in Gravity and Magnetic Applications*. Cambridge University Press. p:461.

18. Nabighian, M.N. **1972**. The analytic signal of two-dimensional magnetic bodies with polygonal cross-section Its properties and use for automated anomaly interpretation. *Geophysics*, 37, pp:507–517.

19. Nabighian, M.N. **1974**. Additional comments on the analytic signal of two-dimensional magnetic bodies with polygonal cross-section. *Geophysics*, 39, pp:85–92.

20. Nabighian, M.N. **1984**. Toward a three-dimensional automatic interpretation of potential field data via generalized Hilbert transforms Fundamental relations. *Geophysics*, 49, pp:780–786.

21. Reid, A. B., J. M. Allsop, H. Granser, A. J. Millet, and W. Somerton. **1990**. Magnetic interpretation in three dimensions using Euler deconvolution, *Geophysics*, 55(1), pp:80–91.

22. Roest, W. R., Verhoef, J. and Pilkington, M. **1992**. Magnetic interpretation using the 3-D analytic signal, *Geophysics*, 57(1), pp:116–125.

23. MacLeod, I.C., Jones, K., and Dai, T.F. **1993**. 3-D analytic signal in the interpretation of total magnetic field data at low magnetic latitudes. *Explor. Geophysics*, 24, pp:679–688.

24. Hsu, S-K., Sibuet, J-C., and Shyu, C-T. **1996**. High-resolution detection of geologic boundaries from potential-field anomalies: An enhanced analytic signal technique. *Geophysics*, 61, pp:373–386.

25. Hsu, S-K., Coppens, D., and Shyu, C-T. **1998**. Depth to magnetic source using the generalized analytic signal. *Geophysics*, 63, pp:1947–1957.

26. Debeglia, N., and Corpel, J. **1997**. Automatic 3-D interpretation of potential field data using analytic signal derivatives. *Geophysics*, 62, pp:87–96.

27. Salem, A. and D. Ravat, **2003**. A combined analytic signal and Euler method (AN-EUL) for automatic interpretation of magnetic data, *Geophysics*, 68(6), pp:1952–1961.

28. Keating, P., and Pilkington, M. **2004**. Euler deconvolution of the analytic signal and its application to magnetic interpretation. *Geophysical Prospecting*, 52, pp:165–182.

29. Nabighian, M., Ander, M., Grauch, V., Hansen, R., LaFehr, T., Li, Y., Pearson, W., Peirce, J.,Phillips, J. and Ruder, M., **2005**. Historical development of the gravity method in exploration.*Geophysics*, 70, pp:63ND–89ND.

30. Heiland C.A. **1940**. *Geophysical exploration*. Prentice-Hall, New York. pp:1036.

31. Bott, M.H.P. **1960**. The use of rapid digital computing methods for direct gravity interpretation of sedimentary basins. *Geophys. J. Roy. Astr. Soc.*, 3:63–67.
32. Williams A. Lima and João B. C. Silva. **2014**. Combined modeling and smooth inversion of gravity data from a faulted basement relief. *Geophysics*, 79(6):F1–F10,
33. Hinze, W. J., Ralph R. B. von Frese and Afif H. Saad. **2012**. *Gravity and Magnetic Exploration. Principles, Practices, and Applications*. Cambridge University Press. pp: 530.
34. Al-Kadhimi, J.A.M., Abbas, M.J. and Fattah, A.S.**1984**. Gravity map of Iraq: SOM Library, Now GEOSURV, Baghdad-Iraq.
35. Al-Bassam, K. S., Bidawi, J. and Al-Kadhimi, J. **1992.** Extension of Hail Arch in Iraq: New findings. *Geosciences and Arab Development*. Number 1, pp:12-13.
36. Jassim, A. Z. and Goff, J. C. **2006**. *Geology of Iraq*. Published by Dolin, Prague and Moravian Museum, Brno, pp:352.
37. Al-Yasi, A. I. **1997**. Use of the potential methods in studying deep geological structures in the western desert - Iraq: Ph.D. Thesis, University of Baghdad, Baghdad, Iraq.
38. Baban, E. N, **2000**, Geophysical study of selected regional lines in the western desert of Iraq: Ph.D. Thesis, University of Baghdad, Baghdad, Iraq.